



# Obeticholic acid prevents carbon tetrachloride-induced liver fibrosis through interaction between farnesoid X receptor and Smad3

Yuan-Yuan Fan<sup>a,1</sup>, Wen Ding<sup>a,1</sup>, Cheng Zhang<sup>b</sup>, Lin Fu<sup>b</sup>, De-Xiang Xu<sup>b,\*</sup>, Xi Chen<sup>a,\*\*</sup>

<sup>a</sup> First Affiliated Hospital, Anhui Medical University, Hefei 230032, China

<sup>b</sup> Department of Toxicology, Anhui Medical University, Hefei 230032, China

## ARTICLE INFO

### Keywords:

Obeticholic acid  
Carbon tetrachloride  
Liver fibrosis

## ABSTRACT

Liver fibrosis results from sustained liver injury and is characterized by inflammation, hepatic stellate cell (HSC) activation, extracellular matrix (ECM) accumulation and liver structure destruction. The Farnesoid-X receptor (FXR) antagonizes toxic liver injury and fibrosis, yet the mechanism in liver fibrosis remains unclear. We investigated the effects of FXR agonist obeticholic acid (OCA) on liver fibrosis in mice. Mice were injected with carbon tetrachloride (CCl<sub>4</sub>) for 3 weeks or 6 weeks to induce liver fibrosis. OCA (5 mg/kg) or PBS is administered daily during CCl<sub>4</sub>-treatment. At sacrifice, biochemical parameters and fibrosis were assessed. Pretreatment with OCA alleviated hepatic injury in 6 weeks group but not in 3 weeks group of CCl<sub>4</sub> liver cirrhosis. At same time, pretreatment with OCA exhibit a dramatic protection of liver fibrosis in both 3 weeks group and 6 weeks group. Further experiments found that OCA pretreatment inhibited  $\alpha$ -SMA expression and the activation of hepatic pSmad3 in 3 weeks group and 6 weeks group of CCl<sub>4</sub>-induced liver cirrhosis. Moreover, OCA activated FXR nuclear translocation and increased the interaction between liver FXR and pSmad3. This led to the discovery of a novel role for FXR in regulating fibrosis through interaction with pSmad3. Our data suggest that CCl<sub>4</sub>-induced liver fibrosis is protected by OCA through interaction between farnesoid X receptor and Smad3.

## 1. Introduction

Liver cirrhosis is currently ranked 11th among the most common causes of death in the world, and is an important reason for disability-adjusted life years and years of life loss, bringing a huge disease burden to the world [1,2]. The cause of liver cirrhosis is due to sustained liver injury induced by different factors, such as alcohol abuse, nonalcoholic steatohepatitis (NASH), hepatitis virus infection, autoimmune liver diseases and hereditary liver diseases [3]. As disease progresses, there is a significant risk of liver fibrosis developing into primary liver cancer, especially hepatocellular carcinoma (HCC) [4–6]. Liver fibrosis results from sustained liver injury and is characterized by inflammation, hepatic stellate cell (HSC) activation, extracellular matrix (ECM) accumulation and liver structure destruction [3]. Among them, the deposition of ECM is the most important reason for liver damage [7]. Two important steps in the ECM process are HSCs activation and conversion

of HSCs to myofibroblasts (MFs) [8,9]. Transforming growth factor (TGF)- $\beta$ 1 is a potent pro-fibrosis regulator that promotes HSC activation and liver fibrosis [10–13]. Moreover, TGF- $\beta$ 1 promotes conversion of HSCs to MFs by activating Smad3 phosphorylation [10,14]. Thus, it is an effective strategy to reduce ECM production by inhibiting the Smad3 pathway to prevent liver fibrosis [15].

FXR, a transcription factor, is mainly expressed in liver, intestine and kidney. Accumulating data demonstrate that FXR regulates, directly or indirectly, a wide program of genes involved mainly in bile acid metabolism, lipid metabolism, glucose regulation and inflammation [16–18]. Obeticholic acid (OCA) is a semisynthetic bile acid derivative and a first-in-class FXR agonist. A study showed that OCA reduced cholic acid secretion and reversed bile flow injury in a rat model of cholestasis [19]. Moreover, OCA was proven to reverse insulin resistance, reduce plasma lipid levels and protect steatosis in an obese rat model [20]. In another experiment, OCA protected against liver injury,

**Abbreviations:** FXR, farnesoid X receptor; OCA, obeticholic acid; CCl<sub>4</sub>, carbon tetrachloride; -SMA,  $\alpha$ -smooth muscle actin; NASH, nonalcoholic steatohepatitis; HCC, hepatocellular carcinoma; HSCs, hepatic stellate cells; ECM, extracellular matrix; MFs, myofibroblasts; TGF- $\beta$ 1, transforming growth factor- $\beta$ 1; ALT, alanine aminotransferase; AST, aspartate aminotransferase; TBA, total bile acid; Co-IP, Co-Immunoprecipitation

\* Corresponding author.

\*\* Correspondence to: X. Chen, Department of Gastroenterology, First Affiliated Hospital, Anhui Medical University, Hefei 230032, China.

E-mail addresses: [xudex@126.com](mailto:xudex@126.com) (D.-X. Xu), [ayfychenxi@163.com](mailto:ayfychenxi@163.com) (X. Chen).

<sup>1</sup> These authors contributed equally to this work.

<https://doi.org/10.1016/j.intimp.2019.105911>

Received 15 July 2019; Received in revised form 5 September 2019; Accepted 12 September 2019

Available online 28 October 2019

1567-5769/ © 2019 Elsevier B.V. All rights reserved.

reduced gut permeability and bacterial translocation in experimental cholestasis [21]. Lately, several researches suggest that FXR has also fibrosis-protect activity [16,22,23]. A recent report showed that chronic treatment with OCA prevented bleomycin-induced pulmonary fibrosis [22]. In addition, OCA reduced thioacetamide-induced hepatic inflammation and fibrosis [23].

Our present research is to be aimed at studying the effects of FXR agonist obeticholic acid (OCA) on liver fibrosis in mice. Our data suggested that OCA pretreatment attenuated HSC activation and liver fibrosis by promoting interaction between hepatic FXR and Smad3. These data suggest that CCl<sub>4</sub>-induced liver fibrosis is protected by OCA through interaction between farnesoid X receptor and Smad3.

## 2. Materials and methods

### 2.1. Chemicals and reagents

Carbon tetrachloride (Item number: 10006480) was from Sinopharm Chemical Reagent Co., Ltd. (Shanghai, China). Obeticholic acid was from Sigma Chemical Co. (St. Louis, MO). FXR (sc-13063) antibody was from Santa Cruz Biotechnologies (Santa Cruz, CA). Lamin A/C (2032S) antibody was from Cell Signaling Technology (Danvers, MA, USA). GAPDH (ab181602), TIMP1 (ab38978) and phospho-Smad3 (ab52903) antibodies were from Abcam (Cambridge, UK). MMP9 (GTX100458) antibody was from GeneTex, Inc. (GeneTex, USA).  $\alpha$ -SMA (A2547) antibody was from Sigma Chemical Co. (St. Louis, MO). Chemiluminescence (ECL) detection kit (K-12043-D10) was from Advansta (Advansta Corporation, CA). Trizol was purchased from Molecular Research Center, Inc. (Cincinnati, Ohio). RNase-free DNase (A3500) and 1-Bromo-3-chloropropane (B9673) were from Promega Corporation (Madison, WI). Serum alanine aminotransferase (ALT), aspartate aminotransferase (AST) and total bile acid (TBA) kits were from Dirui Medical Technology Co., Ltd. (Changchun, China). The hydroxyproline assay kit (A030-2-1) was purchased from Nanjing Jiancheng Bioengineering Institute (Nanjing, China).

### 2.2. Animals and treatments

Eight-week-old male CD-1 mice, weighing 28–32 g, were purchased from Vital River Laboratory Animal Technology Co., Ltd. (Beijing, China). All mice were kept at a 12-h light/dark cycle in temperature of 20–25 °C and humidity of 45–55%. All mice were fed a standard chow with no treatment for a week before experiment. 96 mice were divided into 4 groups (24 mice each group). In CCl<sub>4</sub> alone and CCl<sub>4</sub> + OCA group, mice were intraperitoneally (i.p.) injected with CCl<sub>4</sub> (0.15 ml/kg BW, 20%, dissolved in corn oil) twice a week. In OCA alone and CCl<sub>4</sub> + OCA group, mice were administered with OCA (5 mg/kg, dissolved in PBS) by gavage once per day. The doses of OCA and CCl<sub>4</sub> were referred to previous research [24–26]. Mice were i.p. injected with corn oil and administered with PBS by gavage in control group. Half mice were sacrificed at 3 weeks after the first injection of CCl<sub>4</sub>. The rest mice were sacrificed at 6 weeks after the first injection of CCl<sub>4</sub>. Blood samples were centrifuged (3000  $\times$ g, 15 min) to obtain serum for measurement. Liver sample was taken and frozen immediately in liquid nitrogen then stored in –80 °C refrigerator for the rest experiment. Liver histology samples were collected from left lateral lobe in a square shape and fixed in 4% paraformaldehyde. Mice were anesthetized with a mixture of isoflurane and oxygen and then euthanized followed the humane endpoints principle. We monitored mice 2 times a day during our study. This study was approved by the Association of Laboratory Animal Sciences and the Center Laboratory Animal Sciences at Anhui Medical University (Permit Number: 15-0011). All procedures on animals followed the Guide for the Care and Use of Laboratory Animals (National Institutes of Health Publication No. 85-23, revised 1996).

### 2.3. Biochemical analysis

ALT, AST and TBA were measured using Dirui CS-T300 Chemistry Analyzer (Dirui Medical Technology Co., Ltd., Changchun, China). The liver hydroxyproline content was measured using commercially available assay kits according to the manufacturer's instructions.

### 2.4. Histology and determination of liver fibrosis

Liver tissues were fixed with 4% paraformaldehyde, embedded in paraffin and cut into 5  $\mu$ m thick tissue sections. The tissue sections were stained with hematoxylin and eosin to observe histological manifestations of liver. And Sirius red staining was used to evaluate the extent of liver fibrosis. Hepatic fibrosis was divided into 4 grades (scattered-1, mild-2, moderate-3, and marked-4) according to the percentage of Sirius red positive area. Nine random fields at 200 $\times$  of each sample were selected for scoring. The percentage of Sirius red positive area was quantified using Image-Pro<sup>®</sup> Plus software (Media cybernetics, Inc., version 6.0).

### 2.5. Western blots assay

For total protein extraction, liver lysates were made using 50 mg liver tissues in 500  $\mu$ l protein lysate buffer (added with protease inhibitor and phosphatase inhibitor). For nuclear protein extraction, 200 mg of liver tissues was homogenized with protease inhibitor-containing PBS for 5 times to obtain individual dispersed hepatocytes. Then 500  $\mu$ l pre-cooled PBS containing 0.1% NP-40 was used to lyse the cell membrane. After 1000  $\times$ g, 5 min of centrifugation, the precipitate was collected as the pure nucleus. The nucleus was added to 100  $\mu$ l of protein lysate buffer to release the nuclear protein. After centrifugation at 14,000  $\times$ g for 10 min, supernatant was collected, assayed and denatured. Equal amount of protein (15–40  $\mu$ g) was resolved by SDS-PAGE and transferred to a polyvinylidene difluoride membrane. Membranes were incubated for 12 h at 4 °C using the following specific antibodies: FXR, pSmad3,  $\alpha$ -SMA. The membrane was washed 3 times with DPBS/0.05% Tween-20 and then incubated with secondary antibody for 1–2 h. After washed 3 times in DPBS/0.05% Tween-20 the membrane was then detected by ECL detection kit. The GAPDH level was used as the reference to normalize Values.

### 2.6. Real-time RT-PCR analysis

For total RNA extraction, 50 mg of liver tissue was added to 500  $\mu$ l of TRI reagent to prepare liver tissue homogenate. The homogenate was centrifuged at 12,000  $\times$ g for 10 min to remove the supernatant and added to 100  $\mu$ l of 1-Bromo-3-chloropropane. After shaking for 2 min, the mixture was allowed to stand for 5 min to extract RNA. Then the mixture was centrifuged at 12,000  $\times$ g for 15 min. The supernatant is left as RNA. Isopropanol was added in it to precipitate RNA. Then shook for 2 min and stand still for 10 min. The mixture was centrifuged at 12,000  $\times$ g for 15 min again. The precipitate was taken as RNA. The absorbance ratio at 260 nm and 280 nm was controlled between 1.8 and 2.0 to ensure the purity of the RNA. After RNA was quantified to 500 ng/ $\mu$ l, the RNA was subjected to DNase digestion and reverse transcribed with AMV. GoTaq<sup>®</sup> qPCR master mix and primers (as shown in Table 1) were used to perform real-time RT-PCR. Real-time RT-PCR was carried out using the LightCycler<sup>®</sup> 480 system (Roche Diagnostics GmbH, Mannheim, Germany). Comparative CT method was used to determine the relative mRNA levels. The 18 s level was used as the reference to normalize Values.

### 2.7. Co-Immunoprecipitation (Co-IP)

For Co-Immunoprecipitation, 200 mg of liver tissue was first washed with saline and homogenized with lysis buffer (added with protease

**Table 1**  
Primer sequence for real-time RT-PCR.

Gene	Forward (5' - 3')	Reverse (5' - 3')
18s	GTAACCCGTTGAACCCGATT	CCATCCAATCGGTAGTAGCG
$\alpha$ -sma	GGCTCTGGGCTCTGTAAGG	CTCTTGCTCTGGGCTTCATC
timp-1	CGAGACCACCTTATACCAGCG	ATGACTGGGGTGTAGGCGTA
mmp-2	ACCTGAACACTTCTATGGCTG	CTTCCGCATGGTCTCGATG
mmp-9	GCAGAGGCATACTGTACCG	TGATGTTATGATGGTCCCCTTG

inhibitor and phosphatase inhibitor and without protein denaturant, pH 7.5). The homogenized suspension was centrifuged at  $12,000 \times g$  for 15 min to remove debris. The supernatant was separated and pre-clearing with protein A/G agarose for 5 h at  $4^\circ\text{C}$  on a rocking platform. The mixture was then centrifuged at  $12,000 \times g$  for 30 s. Supernatant was transferred to fresh tubes and add of pSmad3 antibody then incubated at  $4^\circ\text{C}$  on a rocking platform for 3 h. Then added  $50 \mu\text{l}$  of the homogeneous protein A/G-suspension to the mixture and incubate overnight at  $4^\circ\text{C}$ . Then the mixture was centrifuged at  $12,000 \times g$  for 30 s to collect complexes and wash buffer was added to resuspend it. The complexes were washed with wash buffer for 20 min at  $2-8^\circ\text{C}$  for 6

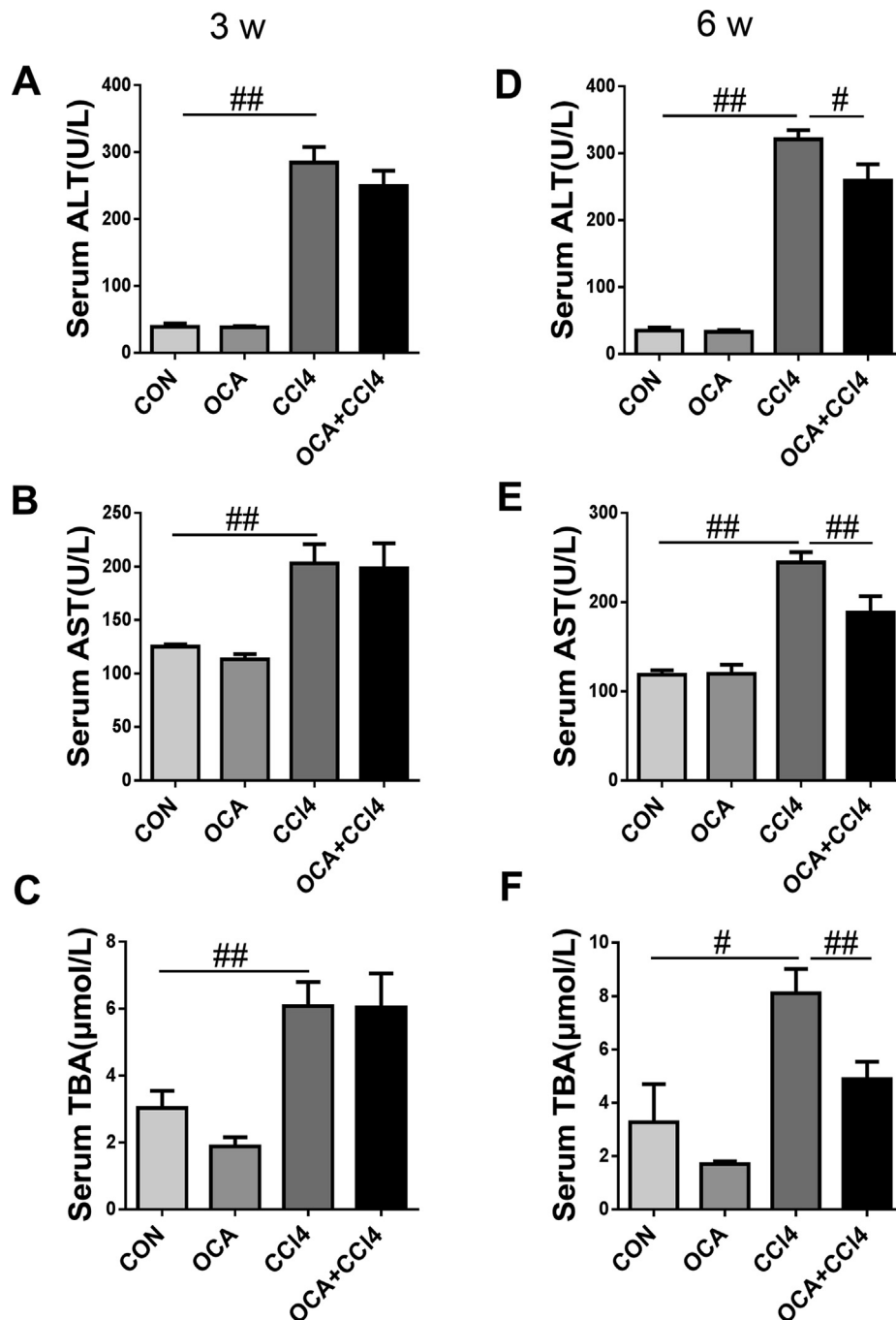


**Fig. 1.** OCA prevents hepatic injury induced by CCl<sub>4</sub>. (A–C) Serum ALT, AST and TBA levels were measured in mice treated with or without OCA at 3 weeks after CCl<sub>4</sub> intraperitoneal injection. (D–F) Serum ALT, AST and TBA levels were measured in mice treated with or without OCA at 6 weeks after CCl<sub>4</sub> intraperitoneal injection. All experiments were repeated for 3 times. Serum samples were collected 1 h after last OCA treatment. Data are expressed as means  $\pm$  S.E.M. (n = 12). \*P < 0.05, \*\*P < 0.01.

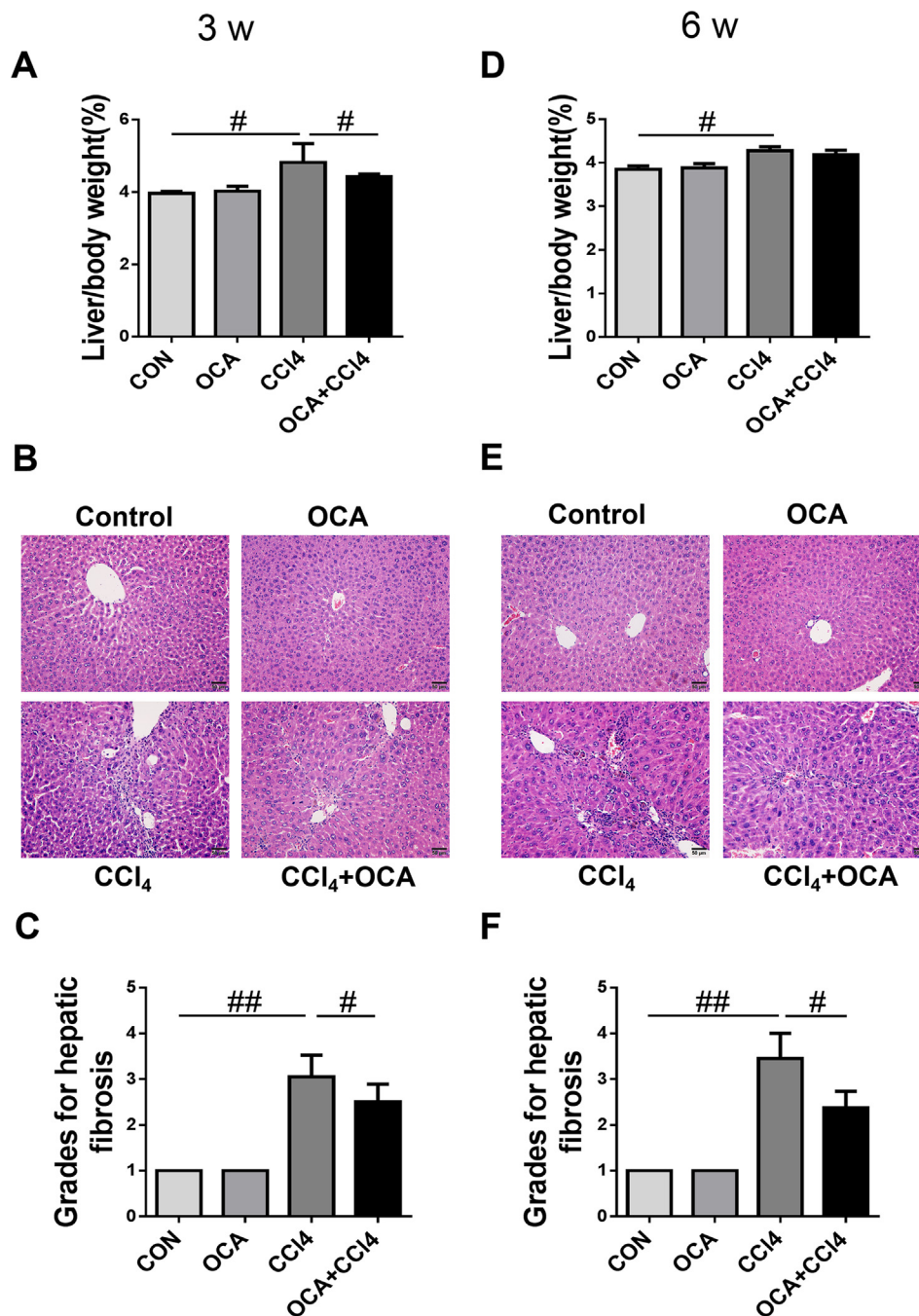


**Fig. 2.** OCA attenuates liver pathological damages and fibrosis scores induced by CCl<sub>4</sub>. (A) Liver/body weight (%) in 3-week groups. (B) Representative H&E staining photomicrographs (magnification: 200×) in 3-week groups. (C) Grades for hepatic fibrosis in 3-week groups. (D) Liver/body weight (%) in 6-week groups. (E) Representative H&E staining photomicrographs (magnification: 200×) in 6-week groups. (F) Grades for hepatic fibrosis in 6-week groups. All experiments were repeated for 3 times. Data are expressed as means ± S.E.M. (n = 12). \*P < 0.05, \*\*P < 0.01.

times. After protein denaturation, the subsequent immunoblotting experiments are the same as 2.5 Western blots.

**2.8. Statistics**

For statistical analysis, data were presented as means ± standard error. Statistically significant differences among different groups were determined by using ANOVA, followed by Student-Newmann-Keuls *post hoc* method. P-value < 0.05 was considered statistically significant. All statistical analyses were performed using SPSS 17.0 statistical software.

**3. Results**

**3.1. OCA prevents liver injury induced by CCl<sub>4</sub>**

Firstly, liver function biochemical indicators were measured. As expected, ALT, AST and TBA were increased 3 weeks after CCl<sub>4</sub> injection (Fig. 1A–C) and remaining increased 6 weeks after CCl<sub>4</sub> injection (Fig. 1D–F). OCA had little effect on the elevation of AST and TBA at 3 weeks after CCl<sub>4</sub> injection and had a tendency to decrease ALT while there was not statistically significant (Fig. 1A–C). This may be due to the protective effect of OCA on liver fibrosis through other mechanisms rather than by direct protection of liver cell damage. And OCA

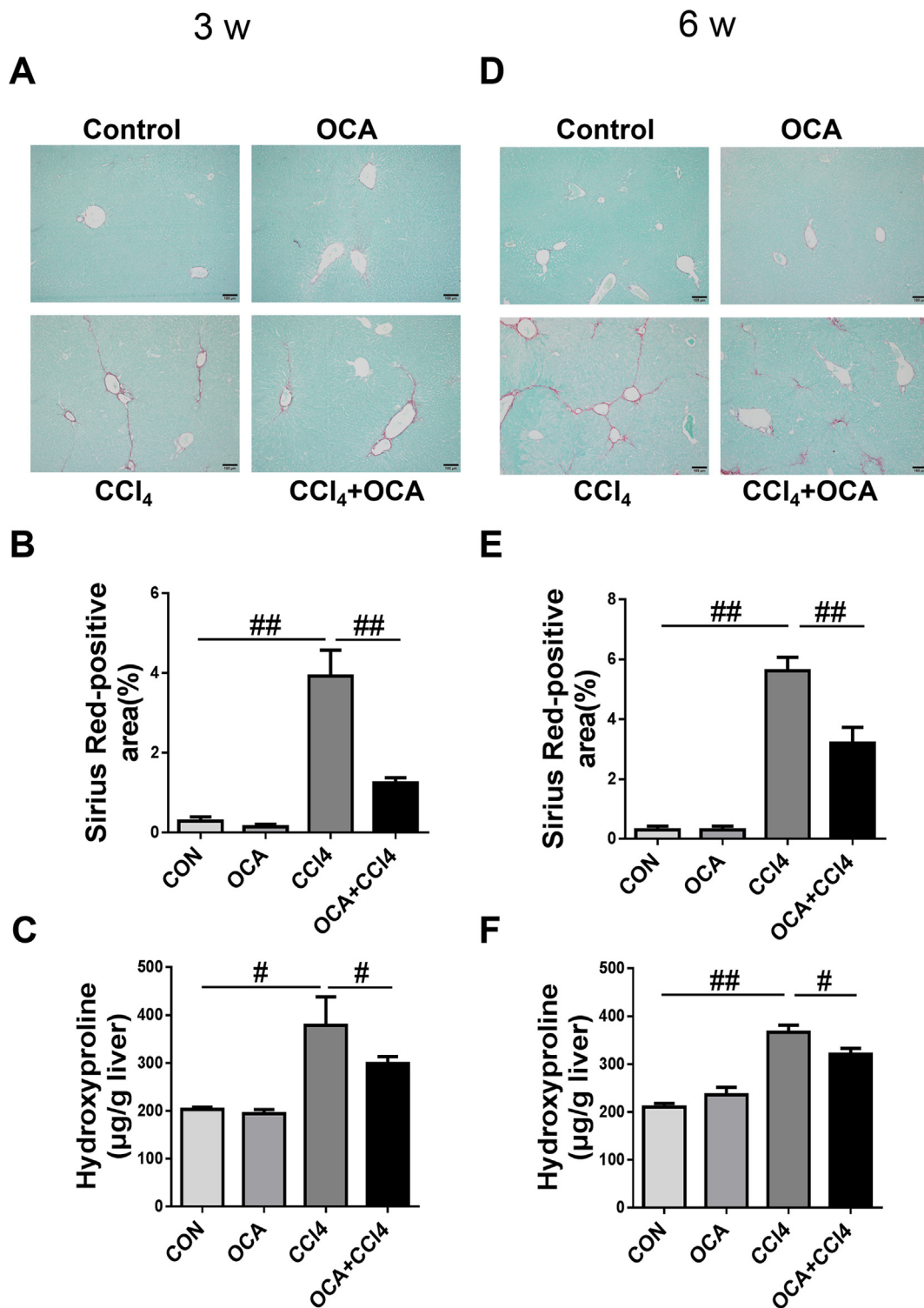


**Fig. 3.** Effects of OCA on CCl<sub>4</sub>-evoked liver fibrogenesis. (A) Representative Sirius staining photomicrographs (magnification: 100×) in 3-week groups. (B) Percentages of Sirius red-positive area in 3-week groups. (C) Content of hepatic hydroxyproline in 3-week groups. (D) Representative Sirius staining photomicrographs (magnification: 100×) in 6-week groups. (E) Percentages of Sirius red-positive area in 6-week groups. (F) Content of hepatic hydroxyproline in 6-week groups. All experiments were repeated for 3 times. Data are expressed as means ± S.E.M. (n = 12). #P < 0.05, ##P < 0.01.

pretreatment slightly alleviated elevation of ALT, AST and TBA 6 weeks after CCl<sub>4</sub> injection (Fig. 1D–F). Similarly, relative liver weight was increased 3 weeks after CCl<sub>4</sub> injection (Fig. 2A) and remaining increased 6 weeks after CCl<sub>4</sub> injection (Fig. 2D). And pretreatment with OCA attenuated elevation of relative liver weight 3 weeks after CCl<sub>4</sub> injection (Fig. 2A). The effects of OCA on histopathology were then

evaluated. Histopathology showed that vascular fraction was disordered, and the hepatic cord was irregularly arranged in CCl<sub>4</sub>-injected mice. In CCl<sub>4</sub> group, light necrotic lesion and moderate inflammatory cell infiltration were observed in liver section. In addition, liver structural damage and pseudolobular formation, characteristic markers of hepatic fibrosis, were shown in the central venous zone and the portal

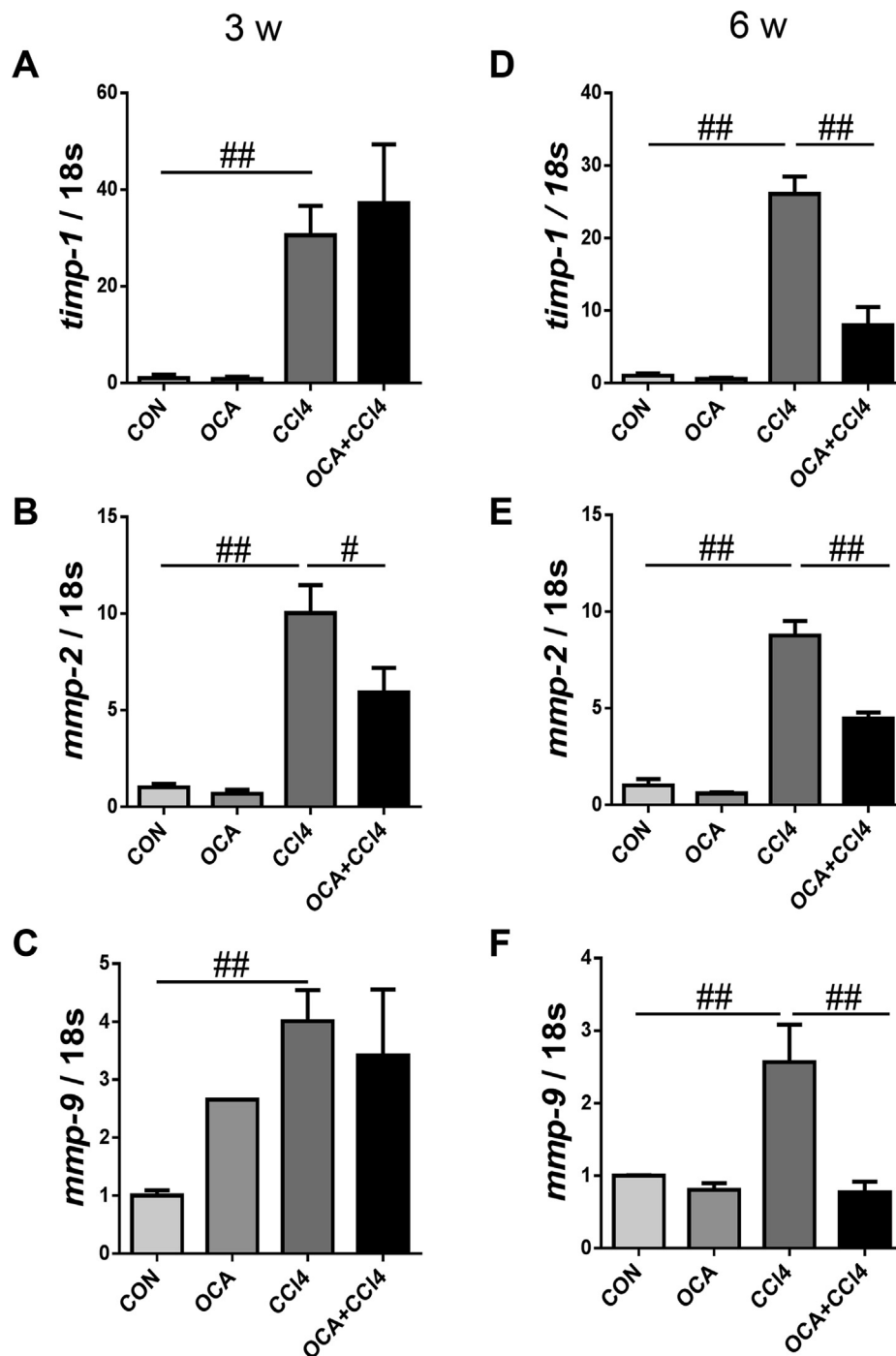


**Fig. 4.** Effects of OCA on CCl<sub>4</sub>-evoked *timp1*, *mmp2* and *mmp9* expression. (A–C) Expression of *timp1*, *mmp2* and *mmp9* in 3-week groups. (D–F) Expression of *timp1*, *mmp2* and *mmp9* in 6-week groups. All experiments were repeated for 3 times. Data are expressed as means ± S.E.M. (n = 12). \*P < 0.05, \*\*P < 0.01.

area of the hepatic lobules (Fig. 2B and E). Interestingly, pretreatment with OCA attenuated liver pathological damage during CCl<sub>4</sub>-induced liver fibrosis (Fig. 2B, C, E, and F).

### 3.2. OCA attenuates liver fibrosis induced by CCl<sub>4</sub>

Subsequently, Sirius red staining was used to evaluate the degree of liver fibrosis that induced by CCl<sub>4</sub>. An obvious collagen accumulation was observed in mouse liver, beginning 3 weeks after CCl<sub>4</sub> injection (Fig. 3A and B) and further increased 6 weeks after CCl<sub>4</sub> injection (Fig. 3D and E). And OCA pretreatment attenuated CCl<sub>4</sub>-induced hepatic collagen matrix accumulation (Fig. 3A, B, D, and E).

Hydroxyproline is an amino acid unique to collagen and is also an important fibrosis marker. Thus, hepatic hydroxyproline content was measured to assess the degree of liver fibrosis. As expected, liver hydroxyproline content was elevated 3 weeks after CCl<sub>4</sub> injection (Fig. 3C) and remaining elevated 6 weeks after CCl<sub>4</sub> injection (Fig. 3F), which was attenuated by OCA pretreatment (Fig. 3C and F).

### 3.3. OCA inhibits hepatic stellate cells activation induced by CCl<sub>4</sub>

Several metalloproteinase genes, expressed by myofibroblasts, were then measured using RT-PCR. As expected, all detected metalloproteinase genes, including *timp-1*, *mmp-2* and *mmp-9*, were upregulated

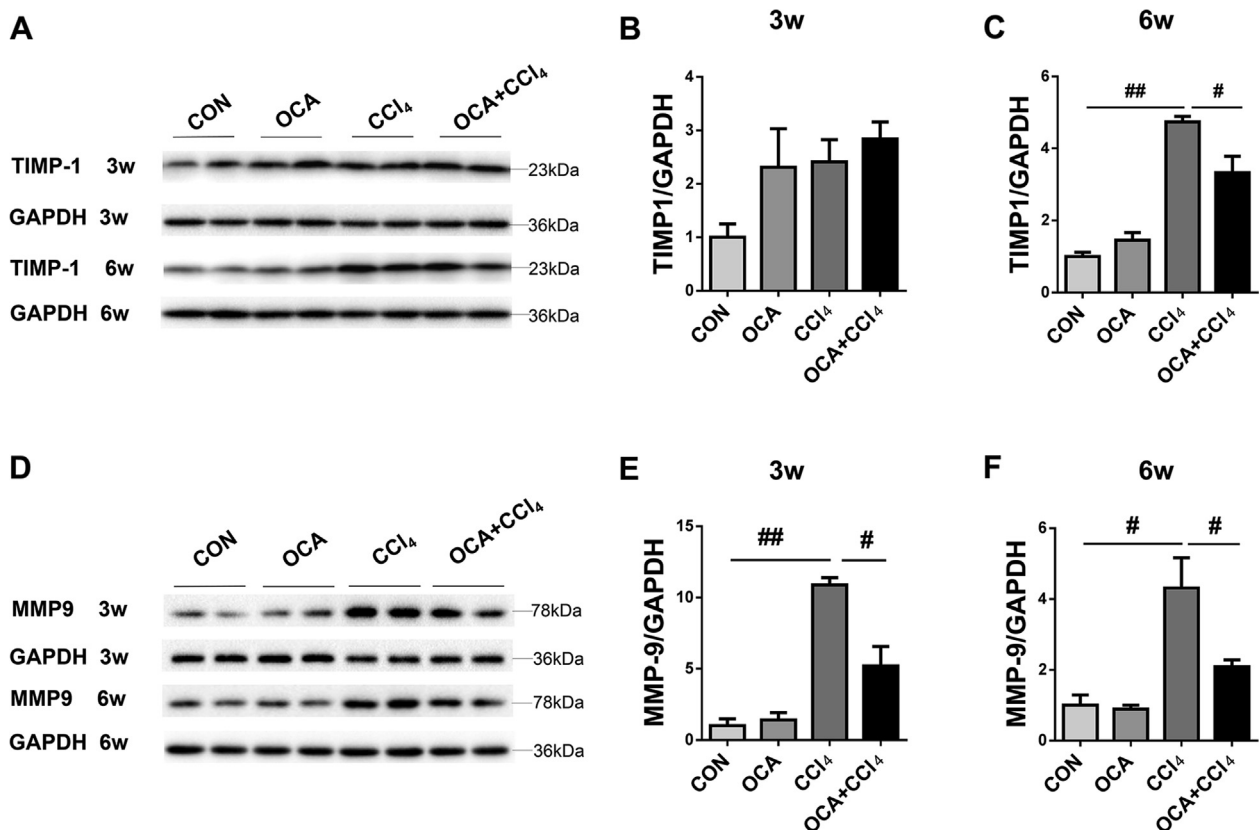


**Fig. 5.** Effects of OCA on CCl<sub>4</sub>-evoked TIMP1, MMP2 and MMP9 expression. (A) Expression and assessment of TIMP1 in 3-week groups and 6-week groups. (B) Expression and assessment of MMP9 in 3-week groups and 6-week groups. All experiments were repeated for 3 times. Data are expressed as means  $\pm$  S.E.M. (n = 12). \*P < 0.05, \*\*P < 0.01.

3 weeks after CCl<sub>4</sub> injection (Fig. 4A–C) and remaining elevated 6 weeks after CCl<sub>4</sub> injection (Fig. 4D–F). And the expression of liver *timp-1*, *mmp-2* and *mmp-9* mRNA was decreased in the OCA-treated 6-week group but the mRNA expression of *timp-1* and *mmp-9* did not change significantly in the OCA-treated 3 weeks group. (Fig. 4B and D–F). Correspondingly, the protein levels of TIMP-1 and MMP-9 was then analyzed using Western blot. As expected, pretreatment with OCA significantly reduced the rise in TIMP-1 and MMP-9 during CCl<sub>4</sub> injection (Fig. 5).  $\alpha$ -SMA is an excellent marker for activated HSCs. As shown in Fig. 6A and B, hepatic  $\alpha$ -SMA protein was analyzed using Western blot. Compared with control group,  $\alpha$ -SMA protein was increased 3 weeks after CCl<sub>4</sub> injection and remaining elevated 6 weeks after CCl<sub>4</sub> injection. At the same time, immunohistochemistry of  $\alpha$ -SMA was performed to more visually observe its expression in liver. As is shown in Fig. 6C and D, hepatic  $\alpha$ -SMA-positive cells was rarely detected in control group. As expected, the number of hepatic  $\alpha$ -SMA-positive cells was increased, beginning 3 weeks and remained elevated 6 weeks after CCl<sub>4</sub> injection (Fig. 6C and D). Interestingly, pretreatment with OCA suppressed CCl<sub>4</sub>-induced upregulation of liver  $\alpha$ -SMA (Fig. 6A and B). Correspondingly, hepatic  $\alpha$ -SMA-positive cells were reduced when mice were pretreated with OCA (Fig. 6C and D).

#### 3.4. OCA inhibits hepatic Smad3 activation induced by CCl<sub>4</sub>

Hepatic Smad3 activation is thought to be one of the most significant mechanism in the pathogenesis of hepatic cirrhosis. Hepatic Smad3 protein activation was analyzed using Western blot. Hepatic pSmad3 level was elevated 3 weeks after CCl<sub>4</sub> injection and remaining increased 6 weeks after CCl<sub>4</sub> injection (Fig. 7A). Interestingly, pretreatment with OCA attenuated hepatic Smad3 phosphorylation 6 weeks after CCl<sub>4</sub> injection (Fig. 7A).

#### 3.5. OCA promotes interaction between hepatic FXR and pSmad3 during CCl<sub>4</sub>-induced liver fibrosis

The intranuclear expression of the FXR was measured to observe the nuclear translocation of FXR. As shown in Fig. 7B, OCA pretreatment obviously increased the expression of the FXR in the nucleus. The interaction between hepatic FXR and Smad3 was then measured using CoIP. As expected, OCA pretreatment increased the level of FXR in the immunocomplexes precipitated by anti-Smad3 antibody (Fig. 7C), suggesting that OCA pretreatment reinforces the physical interaction between hepatic FXR and Smad3 during CCl<sub>4</sub>-induced liver fibrosis.

## 4. Discussion

Previous study has shown that OCA have an anti-inflammatory activity and protect against toxic acute liver injury [26]. To further investigate the effects of OCA on toxic liver fibrosis in mice, we conducted the current experiment. Our results showed that OCA attenuated the elevation of serum ALT, AST and TBA in CCl<sub>4</sub>-induced hepatic fibrosis. Compared with CCl<sub>4</sub> group, lower liver weight, less damage to hepatic structure and less formation of pseudo lobules in liver pathology were observed in OCA-pretreated mice. Hydroxyproline detection and Sirius red staining showed less collagen deposition in OCA-pretreated mice than in CCl<sub>4</sub> group. Our data indicate that OCA prevents CCl<sub>4</sub>-evoked chronic liver injury and liver fibrosis.

It is widely known that activation of HSCs and conversion of HSCs to MFs are the key steps during CCl<sub>4</sub>-induced liver fibrosis [27,28]. Indeed,  $\alpha$ -SMA is a hallmark of activated HSCs. A recent animal experiment showed that pretreatment with OCA down regulated  $\alpha$ -SMA and protected against bleomycin-induced pulmonary fibrosis in rats [26]. Recently, a study found that EDP-305, another FXR agonist,

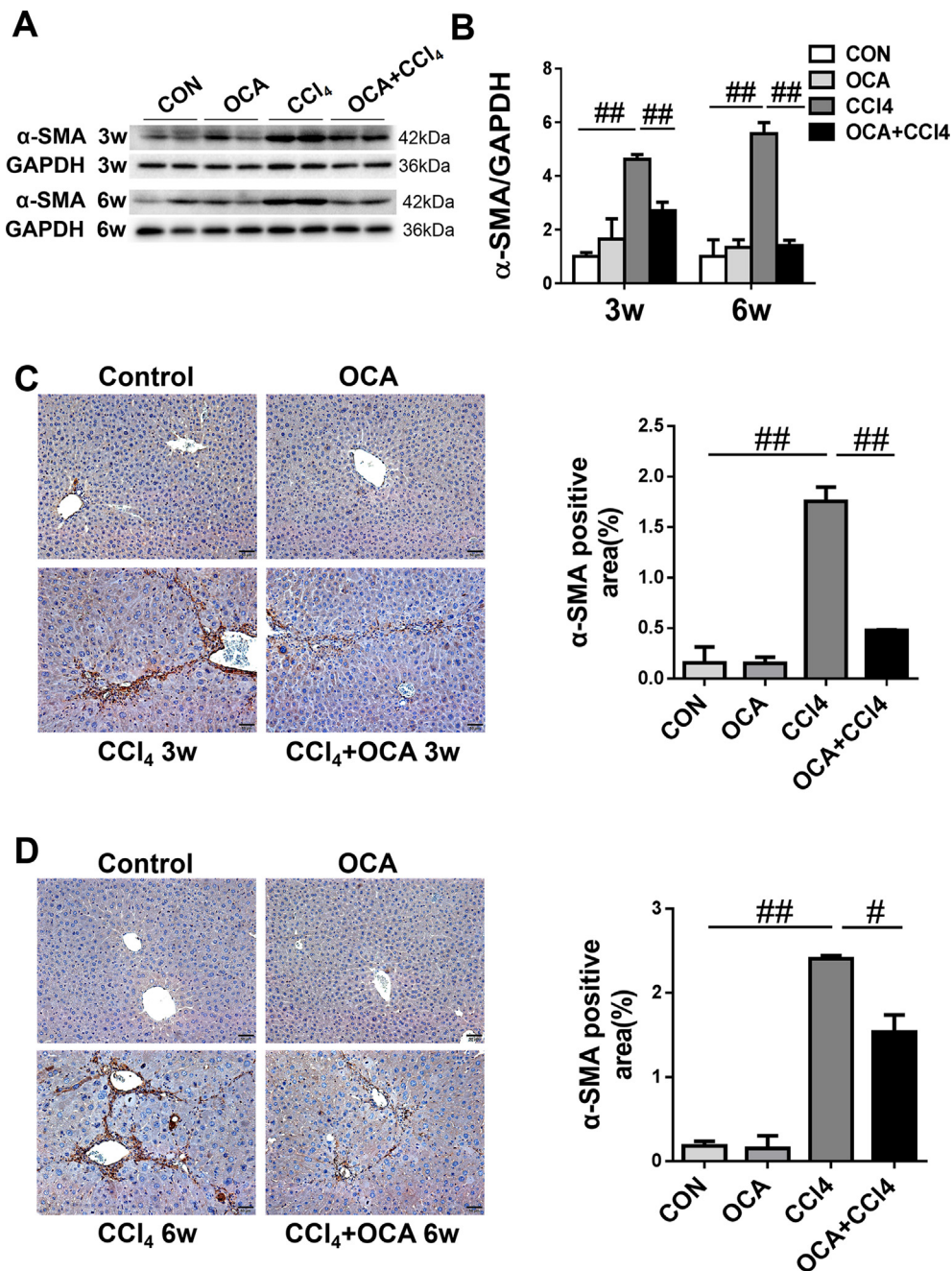


**Fig. 6.** Effects of OCA on CCl<sub>4</sub>-evoked expression of hepatic α-SMA. (A) Hepatic α-SMA protein in different groups were detected by immunoblotting. (B) Assessment of α-SMA levels in 3-week groups and 6-week groups. (C) Representative immunohistochemistry photomicrographs (magnification: 200×) and percentages of α-SMA-positive area in 3-week groups. (D) Representative immunohistochemistry photomicrographs (magnification: 200×) and percentages of α-SMA-positive area in 6-week groups. All experiments were repeated for 3 times. Data are expressed as means ± S.E.M. (n = 12). \*P < 0.05, \*\*P < 0.01.

reduced the expression of α-SMA in interstitial renal fibrosis [29]. Herein, our results showed that hepatic α-SMA expression was up-regulated during CCl<sub>4</sub>-induced hepatic fibrosis, which was almost completely blocked OCA pretreatment. The reduction of hepatic α-SMA expression was confirmed by both western blotting and immunohistochemistry. At the same time, CCl<sub>4</sub> increased the expression of liver *timp-1*, *mmp-2* and *mmp-9* mRNA. Interestingly, the protection of CCl<sub>4</sub>-induced fibrosis by OCA has already occurred in 3w, but the decrease in *timp-1* and *mmp-9* did not occur until 6w. Therefore, we believe that *timp-1* and *mmp-9* may not involve in the main pathway in the protection of CCl<sub>4</sub>-induced fibrosis by OCA. These findings suggest that pretreatment with FXR agonist OCA protects against hepatic fibrosis through inhibiting activation of HSCs and conversion of HSCs to MFs

during CCl<sub>4</sub>-induced chronic liver injury.

Accumulating data have demonstrated that TGF-β1-stimulated activation of Smad3 pathway plays an important role during the process of liver fibrosis [10,11,13]. Therefore, we hypothesize that OCA down regulates hepatic α-SMA expression through blocking Smad2/3 activation in HSCs. As expected, injection with CCl<sub>4</sub> markedly elevated the level of phosphorylated Smad2/3 in mouse liver. Interestingly, pretreatment with OCA attenuated CCl<sub>4</sub>-evoked hepatic Smad3 phosphorylation. The mechanism through which OCA inhibits hepatic Smad3 activation remains obscure. We hypothesize that OCA inhibits hepatic Smad3 phosphorylation by enhancing the interaction between FXR and Smad3. These following results provided important evidence for revealing the important role of FXR in OCA-mediated anti-fibrotic

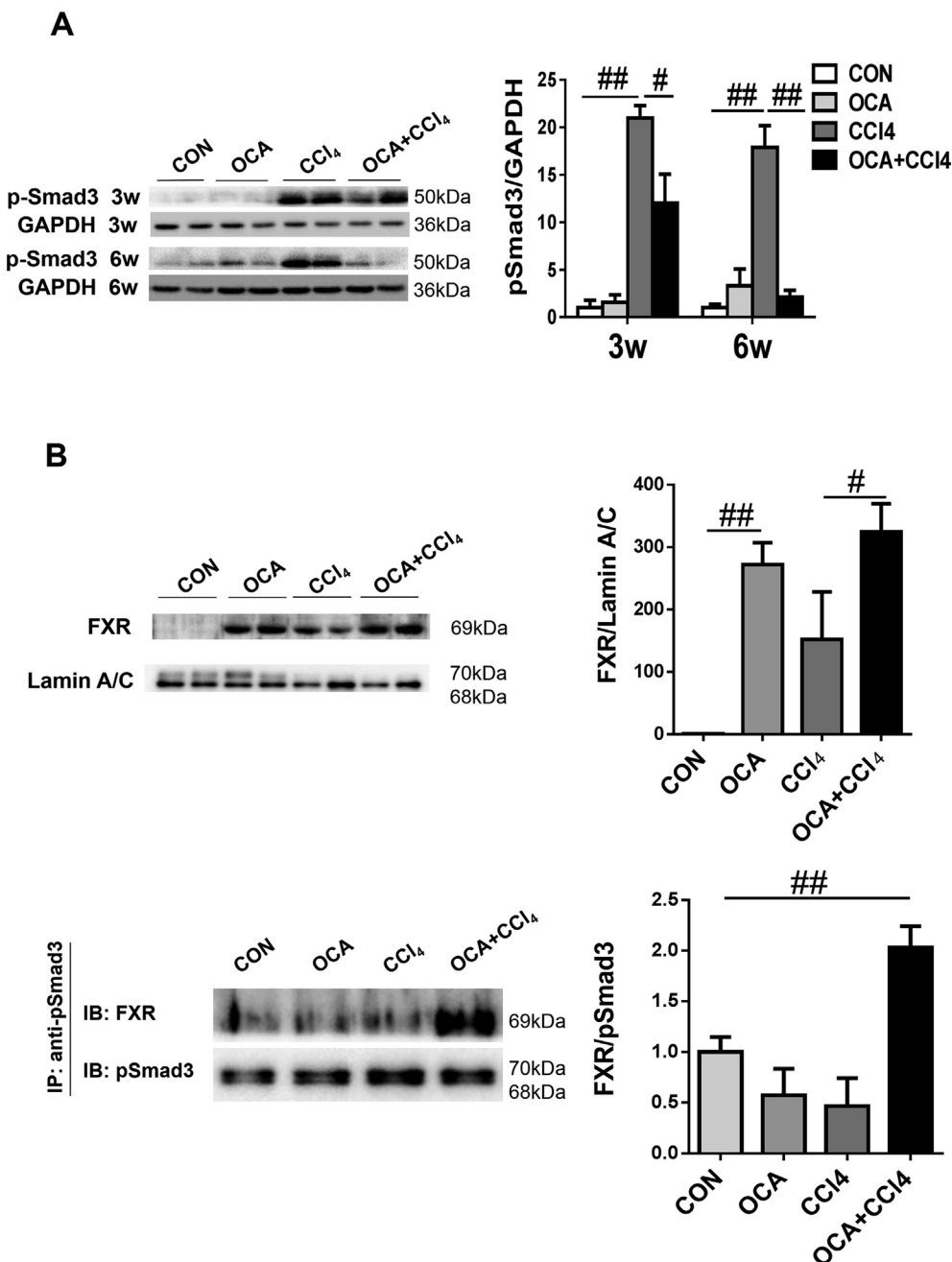


**Fig. 7.** The expression of pSmad3, FXR and interaction between hepatic pSmad3 and FXR. (A) Hepatic pSmad3 protein in different groups were detected by immunoblotting. Assessment of pSmad3 levels in 3-week groups and 6-week groups. (B) Nuclear FXR in 6-week groups was measured using immunoblot. A representative gel for FXR (upper panel) and Lamin A/C (lower panel) was shown. (C) The nuclear fractions were prepared from hepatic and incubated with agarose conjugated either FXR or pSmad3 antibody. FXR and pSmad3 in 6-week groups were measured using immunoblots. All experiments were repeated for 3 times. Data are expressed as means  $\pm$  S.E.M. (n = 12). \*P < 0.05, \*\*P < 0.01.

activity: firstly, pretreatment with OCA promoted translocation of FXR from cytoplasm to nucleus, suggesting OCA could effectively activate hepatic FXR; Secondly, OCA inhibited liver Smad3 phosphorylation induced by CCl<sub>4</sub>. To further investigate the mechanism by which FXR inhibits liver Smad3 phosphorylation, the physical association between hepatic FXR and Smad3 was tested using Co-IP. We showed that OCA reinforced the interaction between hepatic FXR and Smad3. These data suggest that CCl<sub>4</sub>-induced liver fibrosis is protected by OCA through interaction between farnesoid X receptor and Smad3.

Currently, OCA has been registered as an approved drug to treat primary biliary cirrhosis as an agonist of FXR due to its anti-cholesterol property [30]. A double-blind placebo-controlled trial showed that OCA alleviated hepatic inflammation and fibrosis in patients with type 2 diabetes mellitus and nonalcoholic fatty liver disease [31]. Another double-blind placebo-controlled trial indicated that OCA prevented hepatic fibrosis in patients with non-cirrhotic and non-NASH [32]. Recently, data from animal experiments demonstrated that OCA

alleviated steatosis and hepatic fibrosis in a nonalcoholic fatty liver model [33,34]. Another study showed that OCA protected against TAA-evoked fibrosis through its anti-inflammatory activity [23]. Our study found that OCA pretreatment protected CCl<sub>4</sub>-evoked liver fibrosis by suppressing HSC activation. Therefore, FXR agonist OCA may provide a new therapeutic strategy for the clinical development of liver injury and hepatic fibrosis.

Our present research is to be aimed at exploring the effects of FXR agonist obeticholic acid on HSC activation and liver fibrosis. However, some limitations remain in our present study. Firstly, the effects of OCA post-treatment on CCl<sub>4</sub>-evoked hepatic fibrosis were not observed in our present study. Secondly, the impact of OCA on HSC activation and hepatic fibrosis in other animal models has not been evaluated in our present study. Third, our research on the mechanism of OCA protection of CCl<sub>4</sub> is too shallow. Therefore, additional experiments are necessary to further investigate the effects of post-treatment with OCA on CCl<sub>4</sub>-induced HSC activation and hepatic fibrosis. Furthermore, OCA

protection against liver fibrosis needs to be demonstrated in different animal models and the mechanism of OCA on the protective effect of CCL<sub>4</sub>-induced liver fibrosis requires further research.

In summary, the present study investigated the effect of pretreatment with OCA on CCL<sub>4</sub>-induced liver fibrosis in a mouse model. We found that pretreatment with OCA inhibited CCL<sub>4</sub>-induced chronic liver injury and hepatic fibrosis. We provide evidence for the first time that OCA protects against CCL<sub>4</sub>-induced HSC activation and hepatic fibrosis through reinforcing the interaction between hepatic FXR and Smad3. Thus, synthetic FXR agonists including OCA may be a new strategy for treatment of liver fibrosis.

## Acknowledgments

We are grateful to the experimental platform of the Key Laboratory of Environmental Toxicology of Anhui Higher Education Institution. We are grateful for the sponsorship of National Natural Science Foundation of China (81373495), Key Projects of Natural Science Research of Anhui Province in China (KJ2017A202) and Translational Research Institute Research Fund Project of Anhui Province (2017zhxy04). We are grateful to the graduate student Qianqian Chen for the guidance of Sirius Red staining, and the experimental participation of graduate students Xiaopan Gen and Yaqi Wang.

## Funding

This work was supported by the National Natural Science Foundation of China [grant numbers 8137349]; the Key Projects of Natural Science Research of Anhui Province in China [grant number KJ2017A202]; and the Translational Research Institute Research Fund Project of Anhui Province [grant number 2017zhxy04].

## References

- [1] S.K. Asrani, H. Devarbhavi, J. Eaton, P.S. Kamath, Burden of liver diseases in the world, *J. Hepatol.* 70 (2019) 151–171.
- [2] P. Marcellin, B.K. Kutala, Liver diseases: a major, neglected global public health problem requiring urgent actions and large-scale screening, *Liver Int.* 38 (2018) 2–6.
- [3] M. Parola, M. Pinzani, Liver fibrosis: pathophysiology, pathogenetic targets and clinical issues, *Mol. Asp. Med.* 65 (2019) 37–55.
- [4] H.B. El-Serag, Epidemiology of viral hepatitis and hepatocellular carcinoma, *Gastroenterology* 142 (2012) 1264–1273.
- [5] K.A. McGlynn, J.L. Petrick, W.T. London, Global epidemiology of hepatocellular carcinoma, *Clin Liver Dis* 19 (2015) 223–238.
- [6] Z.M. Younossi, A.B. Koenig, D. Abdelatif, Y. Fazel, L. Henry, M. Wymer, Global epidemiology of nonalcoholic fatty liver disease—meta-analytic assessment of prevalence, incidence, and outcomes, *Hepatology* 64 (2016) 73–84.
- [7] P. Ramachandran, J. Iredale, J. Fallowfield, Resolution of liver fibrosis: basic mechanisms and clinical relevance, *Semin. Liver Dis.* 35 (2015) 119–131.
- [8] A. Pellicoro, P. Ramachandran, J.P. Iredale, J.A. Fallowfield, Liver fibrosis and repair: immune regulation of wound healing in a solid organ, *Nat Rev Immunol* 14 (2014) 181–194.
- [9] E. Seki, R.F. Schwabe, Hepatic inflammation and fibrosis: functional links and key pathways, *Hepatology* 61 (2015) 1066–1079.
- [10] Y. Inagaki, I. Okazaki, Emerging insights into transforming growth factor Smad signal in hepatic fibrogenesis, *GUT* 56 (2007) 284–292.
- [11] F. Jiang, G. Liu, G.J. Dusting, E.C. Chan, NADPH oxidase-dependent redox signaling in TGF- $\beta$ -mediated fibrotic responses, *Redox Biol.* 2 (2014) 267–272.
- [12] K. Yoshida, K. Matsuzaki, M. Murata, T. Yamaguchi, K. Suwa, K. Okazaki, Clinicopathological importance of TGF- $\beta$ /phospho-Smad signaling during human hepatic fibrocarcinogenesis, *Cancers* 10 (2018) 183.
- [13] K. Yoshida, M. Murata, T. Yamaguchi, K.M. Zaki, TGF- $\beta$ /Smad signaling during hepatic fibrocarcinogenesis (review), *Int. J. Oncol.* 45 (2014) 1363–1371.
- [14] A.M. Gressner, R. Weiskirchen, Modern pathogenetic concepts of liver fibrosis suggest stellate cells and TGF- $\beta$  as major players and therapeutic targets, *J. Cell. Mol. Med.* 10 (2006) 76–99.
- [15] T. Greuter, V.H. Shah, Hepatic sinusoids in liver injury, inflammation, and fibrosis: new pathophysiological insights, *J. Gastroenterol.* 51 (2016) 511–519.
- [16] L. Adorini, M. Pruzanski, D. Shapiro, Farnesoid X receptor targeting to treat non-alcoholic steatohepatitis, *Drug Discov. Today* 17 (2012) 988–997.
- [17] S. Fiorucci, M. Biagioli, A. Zampella, E. Distrutti, Bile acids activated receptors regulate innate immunity, *Front. Immunol.* 9 (2018).
- [18] P. Lefebvre, B. Cariou, F. Lien, F. Kuipers, B. Staels, Role of bile acids and bile acid receptors in metabolic regulation, *Physiol. Rev.* 89 (2009) 147–191.
- [19] S. Fiorucci, Protective effects of 6-ethyl chenodeoxycholic acid, a farnesoid X receptor ligand, in estrogen-induced cholestasis, *J. Pharmacol. Exp. Ther.* 313 (2004) 604–612.
- [20] S. Cipriani, A. Mencarelli, G. Palladino, S. Fiorucci, FXR activation reverses insulin resistance and lipid abnormalities and protects against liver steatosis in Zucker (fa/fa) obese rats, *J. Lipid Res.* 51 (2010) 771–784.
- [21] L. Verbeke, R. Farre, B. Verbinen, K. Covens, T. Vanuytsel, J. Verhaegen, M. Komuta, T. Roskams, S. Chatterjee, P. Annaert, I.V. Elst, P. Windmolders, J. Trebicka, F. Nevens, W. Laleman, The FXR agonist obeticholic acid prevents gut barrier dysfunction and bacterial translocation in cholestatic rats, *Am. J. Pathol.* 185 (2015) 409–419.
- [22] P. Comeglio, S. Filippi, E. Sarchielli, A. Morelli, I. Cellai, F. Corcetto, C. Corno, E. Maneschi, A. Pini, L. Adorini, G.B. Vannelli, M. Maggi, L. Vignozzi, Anti-fibrotic effects of chronic treatment with the selective FXR agonist obeticholic acid in the bleomycin-induced rat model of pulmonary fibrosis, *J. Steroid Biochem. Mol. Biol.* 168 (2017) 26–37.
- [23] L. Verbeke, I. Mannaerts, R. Schierwagen, O. Govaere, S. Klein, I. Vander Elst, P. Windmolders, R. Farre, M. Wenes, M. Mazzone, F. Nevens, L.A. van Grunsven, J. Trebicka, W. Laleman, FXR agonist obeticholic acid reduces hepatic inflammation and fibrosis in a rat model of toxic cirrhosis, *Sci Rep-Uk* 6 (2016).
- [24] Q. Chen, C. Zhang, M. Qin, J. Li, H. Wang, D. Xu, J. Wang, Inositol-requiring enzyme 1 alpha endoribonuclease specific inhibitor STF-083010 alleviates carbon tetrachloride induced liver injury and liver fibrosis in mice, *Front. Pharmacol.* 9 (2018).
- [25] J. Wang, X. Chen, C. Zhang, L. Tao, Z. Zhang, X. Liu, Y. Xu, H. Wang, J. Li, D. Xu, Phenylbutyric acid protects against carbon tetrachloride-induced hepatic fibrogenesis in mice, *Toxicol APPL Pharm* 266 (2013) 307–316.
- [26] D. Zhang, C. Zhang, J. Wang, B. Wang, H. Wang, Z. Zhang, Y. Chen, Y. Lu, L. Tao, J. Wang, X. Chen, D. Xu, Obeticholic acid protects against carbon tetrachloride-induced acute liver injury and inflammation, *Toxicol Appl Pharm* 314 (2017) 39–47.
- [27] I. Mederacke, C.C. Hsu, J.S. Troeger, P. Huebener, X. Mu, D.H. Dapito, J. Pradere, R.F. Schwabe, Fate tracing reveals hepatic stellate cells as dominant contributors to liver fibrosis independent of its aetiology, *Nat. Commun.* 4 (2013).
- [28] K. Ray, Hepatic stellate cells hold the key to liver fibrosis, *Nat Rev Gastro Hepat* 11 (2014) 74.
- [29] S. Li, S. Ghoshal, M. Sojoodi, G. Arora, R. Masia, D.J. Erstad, D.S. Ferreira, Y. Li, G. Wang, M. Lanuti, P. Caravan, Y.S. Or, L. Jiang, K.K. Tanabe, B.C. Fuchs, The farnesoid X receptor agonist EDP-305 reduces interstitial renal fibrosis in a mouse model of unilateral ureteral obstruction, *FASEB J.* 33 (2019) 7103–7112.
- [30] L. Abenavoli, T. Falalyeyeva, L. Boccuto, O. Tsyryuk, N. Kobyliak, Obeticholic acid: a new era in the treatment of nonalcoholic fatty liver disease, *Pharmaceuticals* 11 (2018) 104.
- [31] L. Abenavoli, T. Falalyeyeva, L. Boccuto, O. Tsyryuk, N. Kobyliak, Obeticholic acid: a new era in the treatment of nonalcoholic fatty liver disease, *Pharmaceuticals (Basel, Switzerland)* 11 (2018).
- [32] B.A.P. Neuschwander-Tetri, R.M. Loomba, A.J.P. Sanyal, J.E.P. Lavine, M.L.M. Van Natta, M.F.M. Abdelmalek, N.P. Chalasani, S.M. Dasarthy, A.M.P. Diehl, B.M. Hameed, K.V.P. Kowdley, A.P. McCullough, N.P. Terrault, J.M.P. Clark, J.P. Tonascia, E.M.P. Brunt, D.E.M. Kleiner, E.M. Doo, C.R.N. NASH, Farnesoid X nuclear receptor ligand obeticholic acid for non-cirrhotic, non-alcoholic steatohepatitis (FLINT): a multicentre, randomised, placebo-controlled trial, *Lancet*, The 385 (2015) 956–965.
- [33] T. Goto, M. Itoh, T. Suganami, S. Kanai, I. Shirakawa, T. Sakai, M. Asakawa, T. Yoneyama, T. Kai, Y. Ogawa, Obeticholic acid protects against hepatocyte death and liver fibrosis in a murine model of nonalcoholic steatohepatitis, *Sci Rep-Uk* 8 (2018).
- [34] H. Jouihan, S. Will, S. Guionaud, M.L. Boland, S. Oldham, P. Ravn, A. Celeste, J.L. Trevisakis, Superior reductions in hepatic steatosis and fibrosis with co-administration of a glucagon-like peptide-1 receptor agonist and obeticholic acid in mice, *MOL METAB* 6 (2017) 1360–1370.